Conclusion

There can be little doubt that magnetism plays a key role in the phase equilibria of systems containing magnetic components. Appreciation of this fact has, however, only emerged in relatively recent times, as shown by the dates of the references to this article. This curious fact can be attributed in no small measure to the "β iron" debate, which took place almost 100 years ago and was eventually settled in favor of "β iron being just the paramagnetic form of α iron" [42]. This formulation satisfied the protagonists at the time but completely ignored the fact that a magnetic transformation is energetically as significant as an ordinary phase transformation!

It is a sobering thought that the phrase, "It's just a magnetic transformation", effectively buried the importance of magnetic transformations, together with the demise of β iron, for more than half a century.

Cited References

1. M. Ko and T. Nishizawa, *J. Jpn. Inst. Met., 43,* 118 (1979).
2. M. Hasebe and T. Nishizawa, *Calphad, 4*(2), 83 (1980).
3. A. H. Qureshi, *Z. Metallkunde, 52,* 799 (1961).
4. G. R. Speich, L. Zwell and K. A. Wriedt, *Trans. AIME, 230,* 939 (1964).
5. M. Ko and T. Nishizawa, *J. Jpn. Inst. Met., 43*(2), 126 (1979).
6. H. Kaneko *et al., IEEE Trans., 13,* 1325 (1977).
7. M. Hansen and K. Anderko, *Constitution of Binary Alloys,* McGraw-Hill (1958), plus Elliott(1965)/Shunk(1969) supplements.
8. T. Nishizawa, M. Hasebe and M. Ko, *Acta Met., 27,* 817 (1979).
9. G. Inden, *Physica, 103B,* 82 (1981).
10. C. Zener, *Trans. AIME, 203,* 619 (1955).
11. A. P. Miodownik, *Calphad, 1(2),* 133 (1977).
12. A. P. Miodownik, Honda Memorial Series, *Invar Alloys,* Chapter 12, Saito, Ed., 228-310 (1978).
13. A. P. Miodownik, Honda Memorial Series, *Invar Alloys,* Chapter 18, Saito, Ed., 429-456 (1978).
14. Y. Nakamura, M. Shiga and S. Santa, *J. Phys. Soc. Jpn., 29,* 210 (1969).
15. G. Inden and W. O. Meyer, *Z. Metallkunde, 66,* 725 (1975).
16. C. T. Peters, Ph. D. thesis, Surrey Univ. (1975).
17. A. P. Miodownik and D. Skinner, International Conference on Martensite Transformations (ICOMAT II), W. Owen, Ed., Cambridge, MA (1979).
18. G. Schlatte and W. Pitsch, *Z. Metallkunde, 66,* 660 (1975).
19. P. R. Swann, W. R. Duff and R. M. Fisher, *Trans. Met. Soc. AIME, 245,* 851 (1969).
20. S. M. Allen and J. W. Cahn, *Acta Met., 24,* 425 (1976).
21. H. Huthmann, Dr. Nat. Thesis Tech. Hosch., Aachen (1977).
22. C. Wagner, *Acta Met., 20,* 803 (1972).
23. G. Inden, *Z. Metallkunde, 68,* 529 (1977).
24. A. P. Miodownik and M. Hillert, *Calphad, 4*(2), 143 (1980).
25. H. Harvig, G. Kirchner and M. Hillert, *Metall. Trans., 3,* 329 (1972).
26. A. P. Miodownik, Th. Henig and L. Lucas, Max-Planck Inst., Stuttgart, unpublished (1979).
27. M. G. Stout *et al., Met. Trans., 8A,* 1316 (1977).
28. J. L. Meijering, *Philips. Res. Rep.,* No. 18, 318 (1963).
29. A. P. Miodownik, *Calphad, 4*(4), 219 (1980).
30. V. Marian, *Ann. Phys., 7*(11), 459 (1937).
31. R. A. Oriani, *Acta Met., 3,* 232 (1955).
32. C. T. Peters and A. P. Miodownik, *Scripta Metallurgica, 7,* 955 (1973).
33. A. Rabinkin, *Calphad J., 3*(2), 77 (1979).
34. J. F. Breedis and L. Kaufman, *Met. Trans., 2,* 2359 (1971).
35. A. P. Miodownik, Thermodynamics Symposium, Münster Univ., unpublished (1972).
36. A. Holden, J. D. Bolton and E. R. Petty, *J. Iron and Steel Institute* (Sept), 721 (1971).
37. H. H. Ettwig and W. Pepperhoff, *Phys. Stat. Solidi., 23*(2), 105 (1974).
38. D. Skinner, Ph. D. thesis, Surrey Univ. (1980).
39. G. Inden, *Z. Metallkunde, 63,* 253 (1972).
40. G. Inden, *Scripta Met., 15,* 669 (1981).
41. G. Inden, *Bulletin of Alloy Phase Diagrams, 2*(4), 412 (1982).
42. M. Cohen, Metallography Symposium, AIME, No. 15, 209 (1965).

The Effect of Continuous Transformations on Phase Diagrams

By Gerhard Inden
Max-Planck-Institut für Eisenforschung GmbH
Max-Planck-Strasse 1, D-4000 Düsseldorf

Alloy phase diagrams usually represent the most stable states of alloys at constant pressure in a temperature-versus-composition diagram. The most important information to be taken from such diagrams is whether the stable states are homogeneous or heterogeneous. Phase boundaries subdivide these diagrams into single- and multiphase regions. Transformations from one single-phase state to another generally occur through intermediate heterogeneous multiphase states. However, there are also transformations that may, but need not, occur through heterogeneous equilibria, e.g., atomic and magnetic order-disorder transformations. The dubious character of that kind of transformation has led to an inadequate representation in phase diagrams. The critical temperatures of these transformations are drawn either as broken lines (thus treating them on the same level as unreliable phase boundaries, e.g., Curie temperatures in ferromagnetic systems such as Co-Ni and Fe-Si [1]) or as a pair of broken lines (thereby tacitly presuming heterogeneous equilibria for these transformations, too; e.g., Co-Fe and Fe-Si [1]). It is the aim of this contribution to suggest an appropriate representation of these order-disorder transformations in phase diagrams, the necessity of which becomes conspicuous by the occurrence of unusual heterogeneous phase equilibria.

These unusual phase equilibria are sharply closing miscibility gaps extending either along a critical temperature line of continuous transformations (thus opening and closing at this line) or starting at the critical temperature and

opening toward lower temperatures. The temperature/composition point at which the gap sharply closes and from which the critical temperature line continues is called a tricritical point [2]. The conditions for the occurrence of such tricritical points have been discussed in general by Landau [3]. Particular cases for atomic and magnetic ordering have been treated in [4–7] and [8–12], respectively.

For the sake of simplicity, this discussion will be confined to binary alloys. The results, however, remain valid for higher component systems, and the transposition to these situations is straightforward.

General Viewpoints

The phase state of an alloy is defined by its physical properties, such as crystal structure, composition, density, viscosity, etc. If these properties do not only apply to the alloy as a whole but also to every subdivision of it, the state of the alloy is *homogeneous*. The state of the alloy is *heterogeneous* if there are subdivisions of the alloy with differing physical properties. By this definition, any change of physical properties produces a change of the state of the alloy.

Among the infinite variety of states, the equilibrium states at fixed values of the variables—pressure, temperature, and composition—are of particular interest. Changes of these variables produce transformations of the equilibrium states. It is very useful to attribute a common denomination to all those states that transform continuously into each other: they all belong to the same *phase state* (or simply phase). The discontinuity in the physical properties is, by definition, a prerequisite for the distinction of phases. Heating a crystalline alloy changes its physical properties, (e.g., the volume by thermal expansion); however, as long as these changes take place continuously, the contracted state at low temperatures and the expanded state at higher temperatures are not designated as different phases. Consequently, homogeneous states of an alloy must be single-phase states. Heterogeneous states of an alloy with continuously varying physical properties, e.g., produced by a concentration gradient, are single-phase states. Heterogeneous states with discontinuously varying properties are multiphase states, and each subdivision of the alloy exhibiting homogeneous properties is usually identified with the corresponding phase.

The physical properties of an alloy can be expressed as derivatives of the molar Gibbs energy,* G; e.g., entropy, $S = -\frac{\partial G}{\partial T}|_p$; volume, $V = \frac{\partial G}{\partial p}|_T$; or specific heat capacity, $c_p = -\frac{\partial^2 G}{\partial T^2}|_p$. This immediately suggests classification of the phase transformations according to Ehrenfest's scheme [13]: a transformation is of nth order if G and its $(n-1)$-order derivatives are continuous and the nth order derivatives change discontinuously at the transformation. A typical second-order transformation would, thus, produce a finite jump of c_p at the transformation.

Model calculations of atomic (bcc, [4, 5]; fcc, [6, 7]) and magnetic [12, 14] order-disorder transformations in alloys predict first- and second-order transformations. In real systems, however, it seems to be accepted that c_p does not take finite values at the transformation. At least for magnetic transformations, this effect has been established experimentally (see [15]). At the Curie temperature, c_p shows a logarithmic singularity. The same behavior can be expected for atomic ordering reactions at the critical temperature of long-range order. In these instances, it is more difficult to decide by experiments whether or not c_p takes finite values at the critical temperature. Ordering reactions are diffusion controlled, and it is difficult to ascertain that equilibrium states are in fact established during the c_p measurements. However, a rise of c_p to infinity for atomic ordering reactions at the critical temperature has been found most recently by Monte Carlo simulations [16]. These "computer experiments" come closest to an ideal experiment. Consequently, Ehrenfest's classification is not applicable to the most general order-disorder transformations, and one should have recourse to a more general classification, such as the one proposed by Tisza [17, 18].

Fortunately, it is not necessary to distinguish second-order from higher-order transformations in phase diagram calculations and representations, because they all produce qualitatively similar contributions to the Gibbs energy. Therefore, it is often sufficient to classify the transformations into *discontinuous* (first-order) and *continuous* (second- or higher-order) *phase transformations,* the continuity or discontinuity being associated only with the physical properties that derive from G by first-order derivatives.

Phase Transformations Under Constraint of Homogeneity. Before considering heterogeneous equilibria, it is very helpful to consider first the equilibria under the constraint of homogeneity. In this instance, each state can be associated with a single phase. The temperature vs. composition diagram indicating the ranges where a given phase is the equilibrium state is called the *configuration diagram.* Different single-phase regions are separated by transformation lines which should be drawn as solid lines for first-order transformations and hatched lines** for higher-order transformations (see Fig. 2).

At first, atomic ordering in a binary alloy $A_{1-x}B_x$ should be considered. The state of order is defined by two different sets of parameters:

- The short-range order (sro) parameters $p_{AB}^{(k)}$, which are defined as the ratio of A-B bonds between k-th neighbors to the total amount of bonds in the alloy, $p_{AB}^{(k)} = \frac{N_{AB}^{(k)}}{\frac{1}{2}z^{(k)}N_L}$,*** where $z^{(k)}$ is the coordination number of the k-th shell and N_L is Avogadro's number (1 mole of alloy).
- The long-range order (lro) parameters p_B^L, which describe the lro by means of the fraction p_B^L of B-atoms on appropriately chosen sublattices, L (see, e.g., [4] and Fig. 1 for bcc and [6] for fcc lattices).

With constant pressure, the equilibrium states minimize Gibbs energy. Because we also maintain the composition

*In this article, all thermodynamic entities will be considered for 1 mole of substance. Therefore, it is not necessary to introduce a special notation for these quantities.

**A hachure for indicating higher-order transformations was first suggested by Swann, Duff, and Fischer in their TEM-work on the ordering in Fe-Al alloys [19].

***$p_{AB}^{(k)}$ takes the value $2x(1-x)$ in the random alloy. Instead of $p_{AB}^{(k)}$, the isotropic "Cowley-Warren short-range order parameters" α_k often are introduced. They are defined as the deviation from the random state: $p_{AB}^{(k)} = 2x(1-x)(1-\alpha_k)$.

Fig. 1 Ordered Atomic Arrangements in bcc Alloys

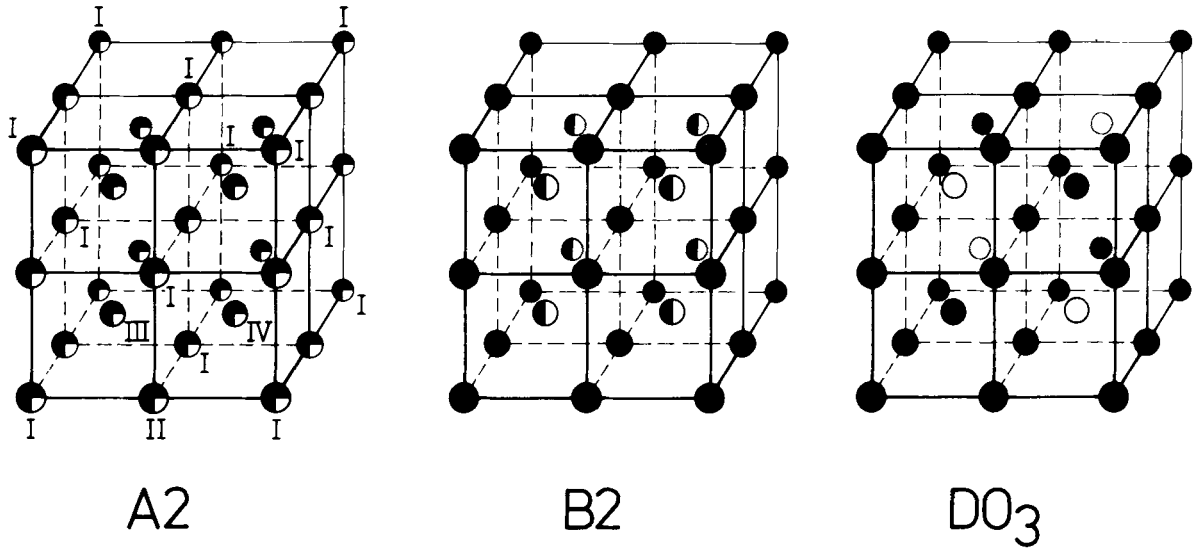

Shown here for a composition $A_{0.75}B_{0.25}$. (**a**) Subdivision of the bcc lattice into four fcc sublattices with parameter twice that of the bcc unit cell. The various long-range ordered structures differ by the occupation of the sublattice positions by *A* and *B*. The random alloy with equally occupied sublattices is represented. The filling of the circles indicates the fraction of *A* (black) and *B* (white) atoms on each position. (**b**) Ordering between nearest neighbors (superstructure *B*2); no ordering between second nearest neighbors. This superstructure admits a stoichiometric composition at $x = 0.5$. (**c**) Ordering between first and second nearest neighbors (superstructure DO_3). This superstructure is stoichiometric at $x = 0.25$, which is detectable from this figure by the complete filling of the sublattice positions I, II, and III by *A* and IV by *B*.

constant, the minimum search of $G = G(T, x, p_B^L, p_{AB}^{(k)})$ need only to be done with respect to the order parameters. This yields the necessary and sufficient conditions:

$$\frac{\partial G}{\partial p_B^L} = 0 \qquad L = 1, 2 \ldots \qquad \text{(Eq 1)}$$

$$\frac{\partial G}{\partial p_{AB}^{(k)}} = 0 \qquad k = 1, 2 \ldots \qquad \text{(Eq 2)}$$

$$d^2G > 0 \qquad \text{(Eq 3)}$$

At high temperatures, Eq 1 admits only the trivial solution $p_B^L = x$, whereas Eq 2 gives the amount of short-range order in dependence on T. The short-range order varies continuously with temperature; therefore, no phase transformation should be associated with these changes. At lower temperatures, two situations are possible and are obtained in model calculations:

- Below a certain temperature there exists a temperature range where Eq 1 and 2 admit two solutions: e.g., one solution with no lro but some sro and a second solution with lro and the corresponding sro. The two solutions correspond to two minima of Gibbs energy; one solution is metastable, the other stable. Then, a temperature, T_0, can be defined at which the Gibbs energies of both solutions are equal (this is the transition temperature of a first-order transition in the configuration diagram). At this temperature, the property of stability or metastability reverses and a phase change with discontinuous changes in the degree of lro and sro (and, consequently, also in enthalpy and entropy) takes place.*

*This, in fact, holds only for the equilibrium states considered here. In reality, some undercooling below T_0 will be necessary to start the transformation by nucleation and growth.

- At temperature T_c, called the critical temperature of lro, one gets $d^2G = 0$. Below this temperature, Eq 1 and 2 again admit two solutions, one stable ($d^2G > 0$), with lro, and the second one unstable ($d^2G < 0$), with no lro. The latter one corresponds to a local maximum of Gibbs energy in the order parameter space. Below the critical temperature of lro $T_c = T^{\text{lro}\rightarrow\text{sro}}$, the degree of lro continuously increases, whereas above T_c no lro, but sro, exists. It is this onset of lro at T_c and its continuous increase below T_c that is indicated by means of the hachure of the T_c line on the low-temperature side (see Fig. 2). The continuous change of lro and sro at T_c implies a continuous change of the enthalpy and the entropy.

At this point, an example is presented, in which the ordering reactions in bcc Fe-Si alloys will be considered. It is known by experiments [20, 21] that ordered atomic arrangements occur in this system between first and second nearest neighbors ($k = 1, 2$). These are denominated as *B*2 and DO_3. The geometric arrangements of Fe and Si atoms in fully ordered structures of these types are shown in Fig. 1 for an alloy with composition $x = 0.25$. In order to obtain the configuration diagram by means of Eq 1 to 3, the Gibbs energy must be known in dependence on p_{Si}^L and $p_{\text{FeSi}}^{(k)}$. For the present purpose of illustration, it is sufficient to consider a highly simplified expression of G as furnished by the Bragg-Williams-Gorsky model because this model already yields the important features under consideration and, furthermore, already provides a surprisingly good description of the experimental findings [22].

In this model, the ordering tendency between the Fe-Si atoms is taken into account by means of the numerical values of the interchange energies $W_{\text{FeSi}}^{(k)}$ between first and

Fig. 2 Calculated Configuration Diagram of Nonmagnetic bcc Fe-Si Alloys

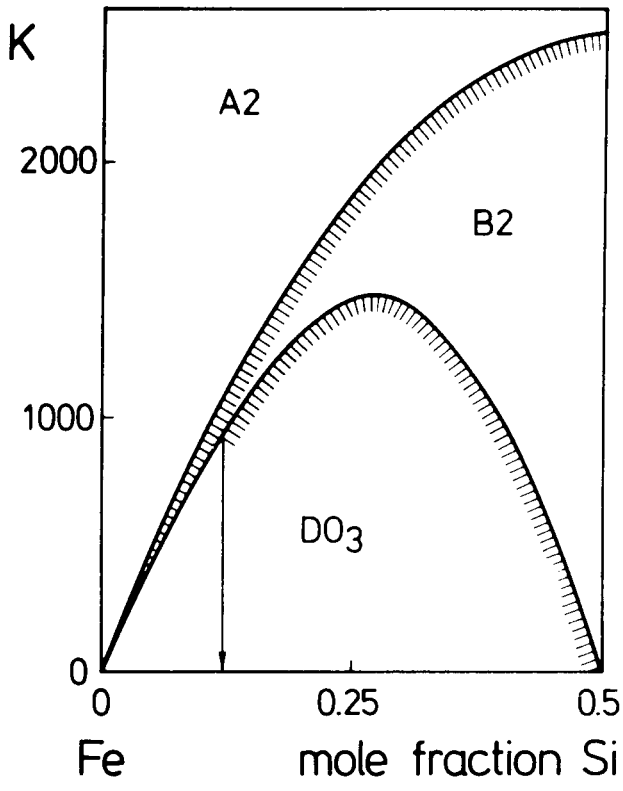

Most stable atomic configurations under the constraint of homogeneity calculated with the Bragg-Williams model, taking first and second nearest neighbor interactions into account. The critical temperatures of continuous transformations (second order in this model) are indicated by a hachure. First-order transformations are indicated by a solid line. In this instance, discontinuous transformations are obtained at $x_{Si} < 0.125$ for the transformation $DO_3 \rightleftarrows B2$.

second nearest neighbors* determined in [23]. The typical approximation and simplification of this model is to replace the short-range order parameters $p^{(k)}_{FeSi}$ by terms of long-range order parameters p^{L}_{Fe} or p^{L}_{Si}.** This necessarily means that no sro is considered in those temperature ranges where lro does not occur, i.e., above the uppermost critical temperature.*** The consequences of this have been discussed in [24].

The minimization of $G = G(T, x, p^{L}_{Si}, W^{(k)}_{FeSi})$ at a given temperature and composition yields the configuration diagram that is shown in Fig. 2. It turns out that the transformation $A2 \rightleftarrows B2$ is second order at all compositions. The transformation $B2 \rightleftarrows DO_3$ shows two kinds of transformations: (a) first-order transformation for $0 \leq x_{Si} \leq 0.124$, and (b) a second-order transformation for $0.124 < x_{Si} \leq 0.5$, as indicated in Fig. 2 by the solid and hatched lines. Of course, in this diagram only bcc states are represented even up to 2000 K because other phases, such as the liquid, have not been considered in the calculation.

Let us now consider magnetic ordering. It is generally accepted that magnetic order-disorder transformations are of second order in pure elements and also in homogeneous alloys. Therefore, the critical temperatures of lro should be represented by hatched lines in the configuration diagrams. This holds for the Curie temperature, T_c (ferromagnetic ordering), and for the Néel temperature, T_N, as well.

Calculation of the Ordering Contributions to the Gibbs Energy. Before removing the constraint of homogeneity, a very simple and accurate method of calculating the lro and sro contributions to the Gibbs energy of homogeneous alloys should be presented. This method is based on an empirically derived expression of the ordering contributions to the specific heat capacity. The advantage of this method over physical models is that no minimization procedure in the order parameter space is required.

The magnetic transformation is particularly appropriate to study the long-range and also the short-range order contributions to the specific heat capacity, c_p, because these transformations are not sluggish as can be the atomic ordering reactions. It could be shown in [12] that the magnetic contribution to c_p can be described below and above T_c by:

$$c_p^{lro} = K^{lro} \cdot R \cdot \ln\frac{1 + \tau^3}{1 - \tau^3} \text{ for } \tau = \frac{T}{T_c} \leq 1 \qquad \text{(Eq 4)}$$

$$c_p^{sro} = K^{sro} \cdot R \cdot \ln\frac{1 + \tau^{-5}}{1 - \tau^{-5}} \text{ for } \tau > 1 \qquad \text{(Eq 5)}$$

where R is the gas constant, and the coefficients K^{lro}, K^{sro} can be evaluated for fcc and bcc structures if the total magnetic entropy, ΔS^{mag}, is known† [12]. This quantity can be derived from the saturation moment per atom of the alloy [25]. The magnetic enthalpy, entropy, and thus, Gibbs energy are obtained from c_p directly by integration [12].††

The advantage of this empirically developed treatment of the magnetic order-disorder contribution to the thermodynamic functions is that both lro and sro contributions can be evaluated easily and accurately. However, the critical temperature and the saturation moment per atom must be known in advance.

This treatment also can be applied to atomic ordering, as pointed out in [12]. Again, the critical temperature of lro

* $W^{(k)}_{FeSi}$ is defined as a difference of bond energies $V^{(k)}_{ij}$: $W^{(k)}_{FeSi} = -2V^{(k)}_{FeSi} + V^{(k)}_{FeFe} + V^{(k)}_{SiSi}$

** Introducing the four fcc sublattices, L = I, II, III, IV (see [4] and Fig. 1), one sets approximately:

$$p^{(1)}_{FeSi} = \tfrac{1}{4}[(p^{I}_{Fe} + p^{II}_{Fe})(p^{III}_{Si} + p^{IV}_{Si}) + (p^{I}_{Si} + p^{II}_{Si})(p^{III}_{Fe} + p^{IV}_{Fe})]$$

$$p^{(2)}_{FeSi} = \tfrac{1}{2}[p^{I}_{Fe}p^{II}_{Si} + p^{I}_{Si}p^{II}_{Fe} + p^{III}_{Fe}p^{IV}_{Si} + p^{III}_{Si}p^{IV}_{Fe}]$$

*** In this situation, $p^{L}_{Fe} = x_{Fe}$ and $p^{L}_{Si} = x_{Si}$, and consequently $p^{(1)}_{FeSi} = p^{(2)}_{FeSi} = 2x_{Fe}x_{Si}$, which is the value for the completely random alloy.

† $K^{lro} = \frac{12}{\pi^2}\frac{\Delta S^{mag}}{R} - \frac{3}{5}K^{sro}$, $K^{sro} = \frac{\Delta S}{R} \cdot \frac{\frac{12}{\pi^2} \cdot A \cdot V}{B - V(B - \frac{3}{5}A)}$

where $V = 0.4$ for bcc alloys; $V = 0.28$ for fcc alloys; $A = 0.64527561$; and $B = 0.59787726$.

†† The integration of Eq 4 and 5 yields a complicated expression with transcendental functions. In order to stick with a power series representation, M. Hillert has proposed to expand Eq 4 and 5 by a truncated Taylor series [53].

and the total entropy of transformation $\Delta S^{order \rightarrow disorder}$ must be known in advance.

It can be concluded, therefore, that once the critical temperatures of lro are known, the Gibbs energy contributions should be calculated by means of the c_p-formalism. The critical temperatures of lro can be taken from experiments if available, or from model calculations such as those presented in [4–7]. It is the merit of model calculations such as those used previously that they allow the prediction (or interpolation or extrapolation) of critical temperatures. Thus, both methods are complementary.

Transformations Without Constraint of Homogeneity (Phase Diagrams). Having so far considered the most stable states of an alloy with the constraint of homogeneity, the removal of this constraint will allow heterogeneous states to occur if they are more stable. Each of the different phases which then are in equilibrium with each other must, of course, be in their most stable state under the constraint of homogeneity. This situation arises if Gibbs energy is concave with respect to composition in a composition interval, and the contact points of the tangent to the Gibbs energy yield the compositions x_1 and x_2 of the two phases in equilibrium.

The compositions x_1 and x_2 indicate the boundary of heterogeneous equilibria. Outside these composition ranges, the most stable states of the alloy are the same as those obtained under the constraint of homogeneity.

Therefore, the phase diagrams are identical with the configuration diagrams in those temperature and composition ranges where single-phase states are most stable. The critical temperatures should be indicated in the same fashion in both diagrams. In the regions of heterogeneous equilibria, the critical temperatures must be replaced by phase boundaries in the phase diagram. A first-order transformation occurring under the constraint of homogeneity always implies heterogeneous equilibria when the constraint is removed. Therefore, in phase diagrams, only phase boundaries of heterogeneous equilibria and critical temperatures of continuous transformations will appear. The inverse is not true: heterogeneous equilibria are not exclusively induced by first-order transformations; they also can be induced by higher-order continuous transformations, which already has been pointed out long ago by Landau [3]. This will now be illustrated with three examples, one for atomic and two for magnetic ordering.

"In Phase Transformations Under Constraint of Homogeneity", the atomic ordering in bcc Fe-Si alloys has been treated with the Bragg-Williams model. The Gibbs energy of the most stable homogeneous states has been obtained with dependence on temperature and composition. Let us now remove the constraint. The result of the shape analysis of Gibbs energy yields the phase diagram in Fig. 3. Comparing this with Fig. 2, it can be seen that the two-phase field $B2 + DO_3$ in the phase diagram extends beyond the temperature range of discontinuous transformations shown in the configuration diagram. The miscibility gap ends at a sharp point, from which the second-order critical temperature starts as continuation. This unusual closing of a miscibility gap is typically produced by higher-order transformations. Fundamental thermodynamic rules would be violated if the second-order transformation were not indicated in the phase diagram.

This peculiarity can be even better illustrated by means of a magnetic transformation. Let us consider a binary fcc system with a ferromagnetic component A and a nonmagnetic component B. The Curie temperature is assumed to vary linearly from a value 1000 K for A to 0 K at B. Similarly, we presume a linear decrease of the mean atomic moment from 2 μ_B at A to 0 μ_B at B. Finally, no preferential atomic bonds between like or unlike atom pairs are presumed, i.e., an ideal solid solution. The configuration diagram is very simple, showing only the critical temperature T_c of magnetic lro, Fig. 4(a). The Gibbs energy of the homogeneous alloy consists of two parts, the ideal solution part and the magnetic part, which can be evaluated with the c_p-method mentioned in "Calculation of the Ordering Contributions to the Gibbs Energy". The analysis of the shape of the resulting Gibbs energy function yields the phase diagram in Fig. 4(b), which shows a magnetically induced miscibility gap. Here, a ferromagnetic and a paramagnetic phase with different compositions are in equilibrium with each other. Again, the very typical closure of the miscibility gap is obtained.

A second example with two ferromagnetic components might be of interest, too. Again, a binary fcc system with ideal solution behavior of the chemical terms is considered, the Curie temperature is assumed to vary linearly with composition, as shown in the configuration diagram (Fig. 5a), and the mean magnetic moment per atom is assumed to vary linearly from 2 μ_B in A to 1 μ_B in B. The resulting phase diagram is shown in Fig. 5(b). In a limited composition range, the magnetic transformation produces

Fig. 3 Calculated Phase Diagram of Nonmagnetic bcc Fe-Si Alloys

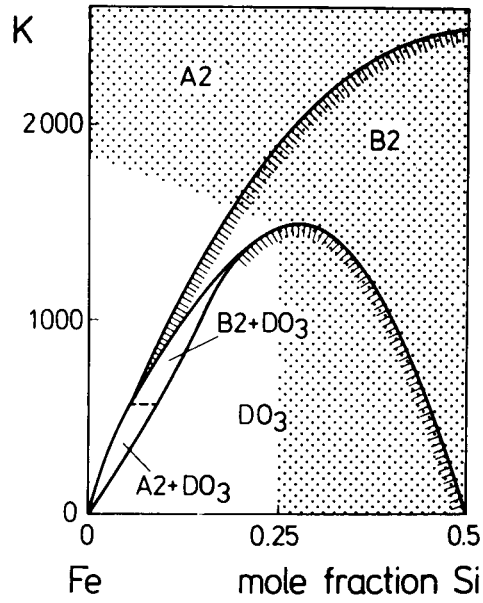

Most stable states without constraint of homogeneity, derived from the same calculations as in Fig. 2. Heterogeneous equilibria appear not only along the first-order transformation line in Fig. 2 but also along its second-order continuation. The miscibility gap $B2 + DO_3$ terminates at a sharp critical point. Such sharply closing miscibility gaps were not consistent with thermodynamic rules if the second-order transformation line were omitted. The shaded area indicates the temperature and composition ranges where bcc equilibria cannot be observed experimentally.

Fig. 4 Configuration and Phase Diagram of Hypothetical Binary Alloy *A-B* with Ferromagnetic Component *A* and Nonmagnetic Component *B*

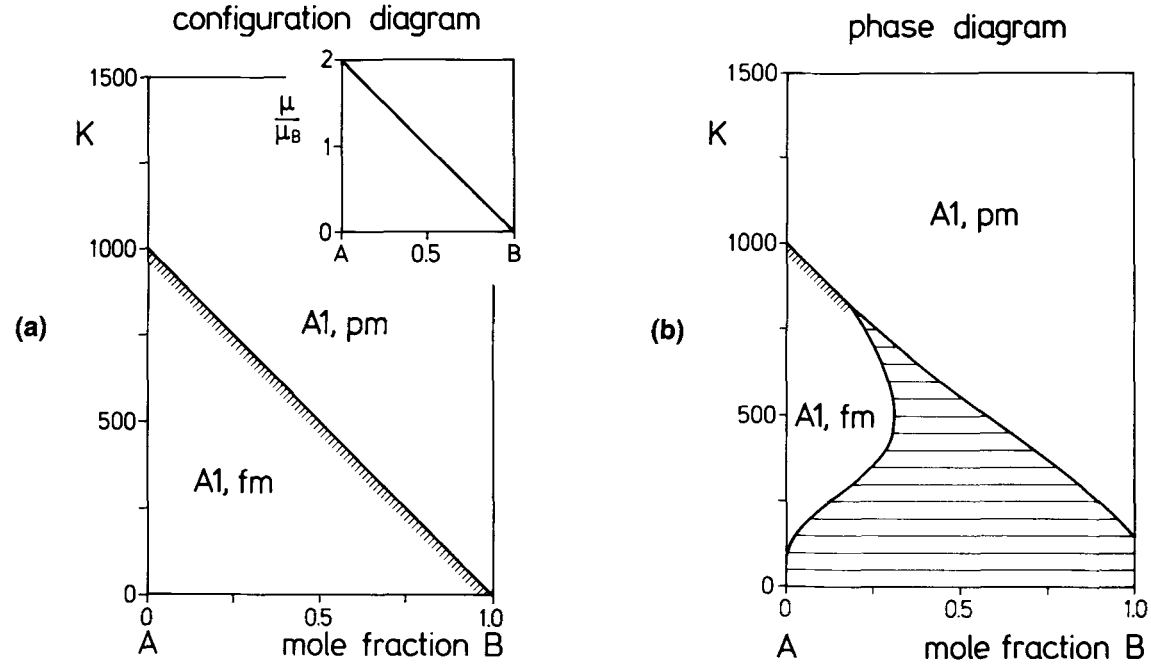

The alloy is assumed to be an ideal solution with respect to the atomic interactions. The fcc crystal structure (*A*1) is assumed at all compositions. (**a**) Configuration diagram showing the assumed continuous magnetic transformation. The inset shows the assumed composition variation of the mean magnetic moment per atom. (**b**) Phase diagram showing a magnetically induced miscibility gap; a ferromagnetic and a paramagnetic phase are in equilibrium with each other for compositions and temperatures within the heterogeneous phase field.

Fig. 5 Configuration and Phase Diagram of Hypothetical Alloy *A-B* with Ferromagnetic Properties at All Compositions

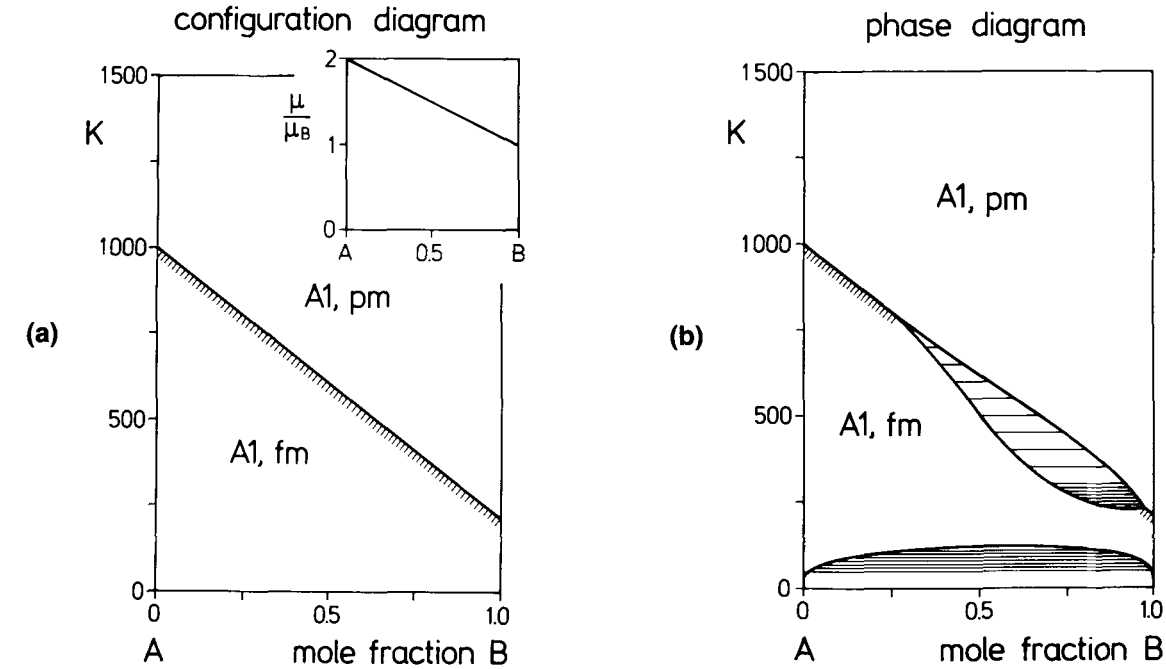

An ideal solution, with respect to the atomic interactions, and the fcc crystal structure (*A*1) at all compositions are assumed. (**a**) Configuration diagram showing the assumed continuous magnetic transformation. The inset shows the assumed composition variation of the mean magnetic moment per atom. (**b**) Phase diagram showing a heterogeneous transformation in the range of the Curie temperature.

Fig. 6 Calculated Phase Diagram of bcc Fe-Si Alloys with $x_{Xi} \leq 0.25$

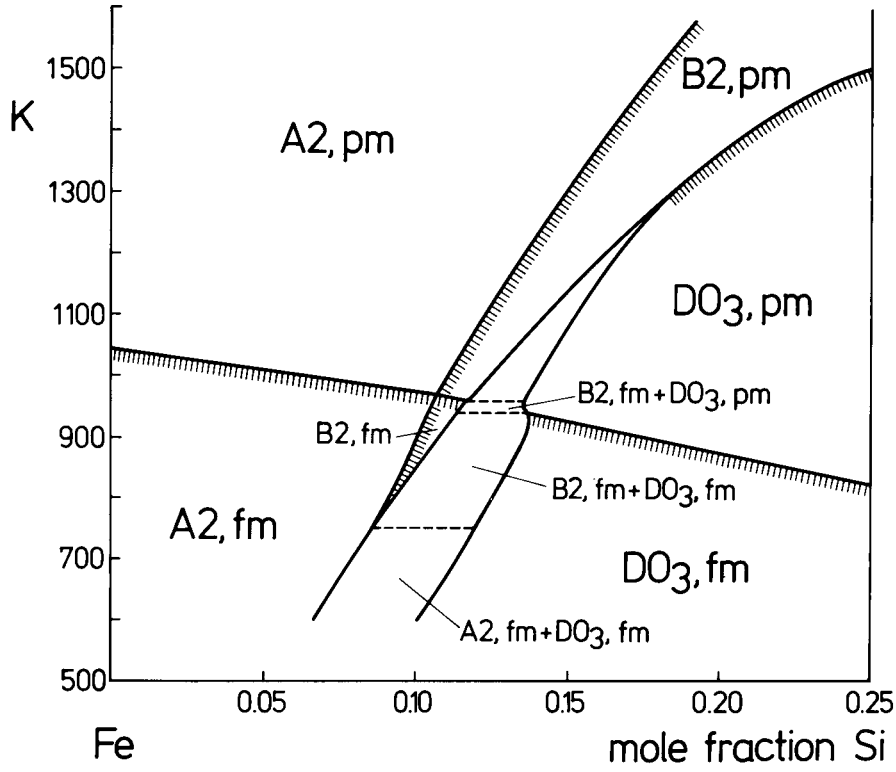

The calculation has been made with the Bragg-Williams model, taking into account chemical interactions between first and second nearest neighbors and magnetic interactions between nearest neighbors. Spin 1 was assumed for the Fe-atoms and no magnetic moment for the Si-atoms. Magnetic interactions were considered between first nearest neighbors.

heterogeneous equilibria just like the liquid/solid transformation in alloys, although the transformation is of higher order under the constraint of homogeneity.

Of course, these findings depend on the particular physical properties of the alloy system, which have been presumed here. At this stage, it should not be discussed whether or not these assumptions are realistic, i.e., applicable to a real alloy system. However, these examples clearly show that higher-order transformations in homogeneous alloys can produce quite the same heterogeneous equilibria as first-order transformations.

Applications

The preceding discussion was essentially based on calculations of phase equilibria. Experimental results have been discarded so far. This was intentional. It is the advantage of the model calculations that there is no doubt about the character of the transformations in homogeneous alloys and that the equilibrium state can be defined precisely, whereas in experiments it can happen that metastable instead of stable states are observed. The choice of the Bragg-Williams model was not purely a matter of convenience. This rather simple model is applicable to complicated systems, and it already provides a very accurate description of the experimental findings if appropriate corrections for sro effects are applied [24]. In practical situations, it may turn out to be difficult to distinguish a very narrow two-phase field from a homogeneous second- or higher-order transformation. Then it will be of great help to know whether or not the model calculations predict first order, or whether or not a higher-order transformation should produce heterogeneous equilibria. Such circumstances will now be considered.

The bcc equilibria in Fe-Si alloys already have been discussed in the previous section, with respect to atomic ordering. In the real system, magnetic interactions also need to be considered, because the alloys are ferromagnetic. The Curie temperature, T_c, crosses the critical temperatures of lro $T^{DO_3 \rightarrow B2}$ and $T^{B2 \rightarrow A2}$, leading to mutual influence of atomic on magnetic ordering, and vice versa. It has been shown in [12] and [26] that such mutual influences can be treated with the Bragg-Williams model. In order to get a guide line for the equilibria in this system, the calculation of the phase diagram has been made, which is shown in Fig. 6, for the composition range $0 \leq x_{Si} \leq 0.25$.* The experimental results are shown in Fig. 7. Both diagrams agree surprisingly well. The most striking discrepancy is with concern to the transformation $D0_3 \rightleftarrows B2$ at tempera-

*This diagram differs slightly from the one in [26], which was calculated using spin 1/2 for the Fe atoms. The present diagram was calculated taking into account spin 1 for Fe and a small magnetic energy contribution from Fe-Si pairs. The energy parameters were:

$W^{(1)}_{FeSi} = 2830\ k$, $W^{(2)}_{FeSi} = 1410\ k$, $x = 0.71$

$J^{(1)}_{FeFe} = -244\ k$, $J^{(1)}_{FeSi} = -45\ k$, $\mu = 0.8$

For notation and units, see [12].

Fig. 7 Experimentally Determined Phase Diagram of bcc Fe-Si Alloys with $x_{Si} \leq 0.25$

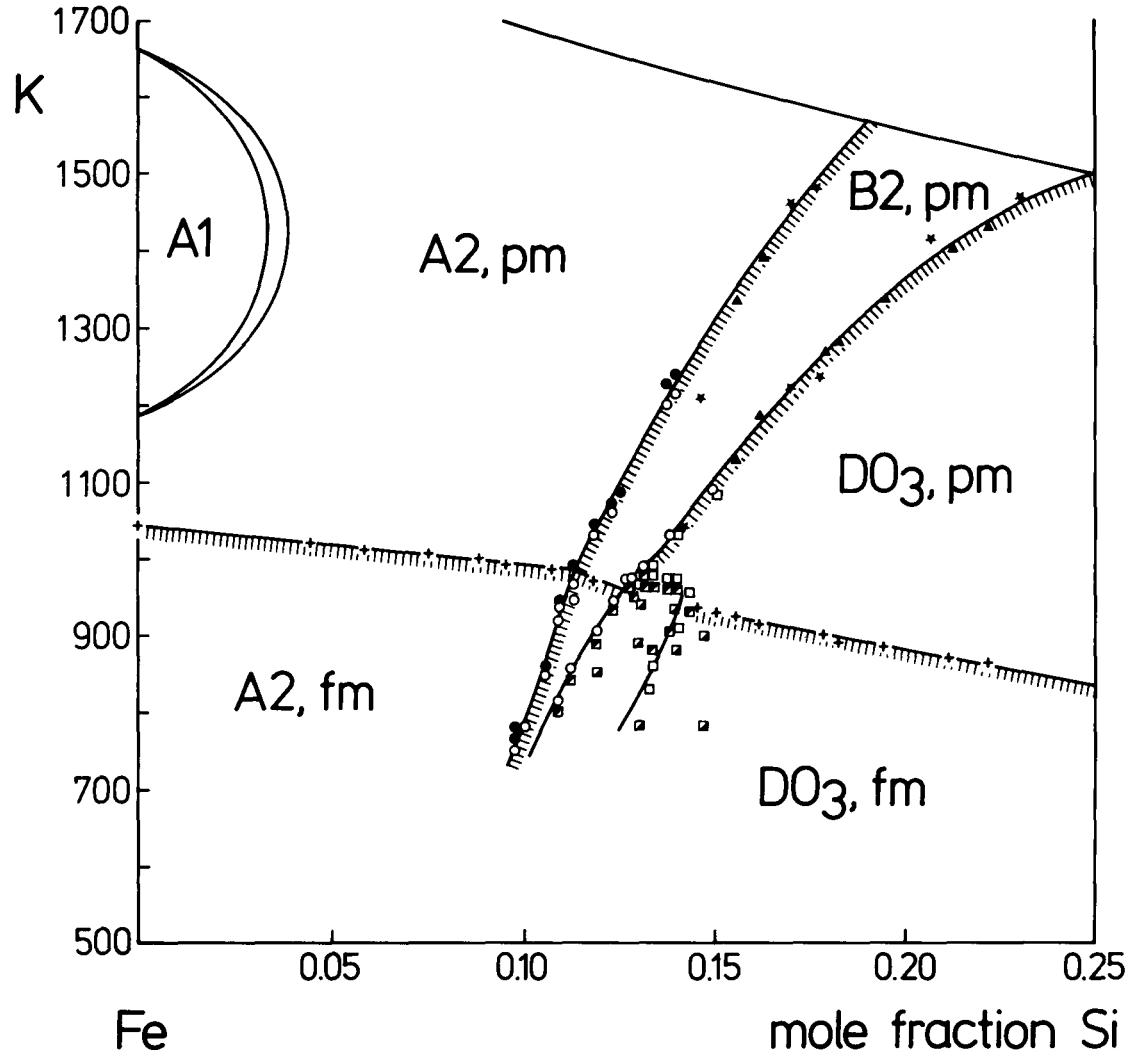

★ ≡ High-temperature neutron diffraction [20]; ● ≡ Homogeneous $A2$, TEM [21]; ○ ≡ Homogeneous $B2$, TEM [21]; □ ≡ Homogeneous DO_3, TEM [21]; ◩ ≡ $B2 + DO_3$, TEM [21]; ◪ ≡ $B2 + DO_3$, TEM [27]; and +, ▲ ≡ c_p [28].

tures above T_c, where the model predicts heterogeneous equilibria, whereas careful electron microscopic observations [21, 27] have shown that, above the Curie temperature, the transformation $DO_3 \rightleftarrows B2$ is homogeneous (therefore, the hatched transformation line in the experimental diagram). At temperatures below T_c, a miscibility gap with $B2$ and DO_3 ordered phases in equilibrium has been found. In [22], the magnitude of the thermodynamic driving force for the phase separation has been evaluated with the model calculations. Above T_c, this driving force turns out fairly small, probably too small* to supply the inevitable coherency strain and interface energies required for the incipient process of a heterogeneous microstructure formation. Below T_c, the driving force is nearly doubled by the magnetic contributions. There, the predicted heterogeneous equilibria could be confirmed experimentally. In [2], this is discussed in detail for the very similar alloy system Fe-Al.

The full phase diagram, based on experimental results, is shown in Fig. 8. The non-bcc equilibria have been taken from the literature [29]. Recent findings on a further transformation within the DO_3 phase field [30] have not been incorporated in this diagram, because the transformation needs further elucidation; this transformation could not be identified in high-temperature diffraction experiments [20]. Furthermore, the very similar findings reported for Fe-Al alloys [31] could not be identified in high-temperature diffraction experiments or in c_p-measurements [32], although heat effects should be detectable near the transformation temperatures [31], whereas the expected effects due to atomic disordering could clearly be detected in these experiments. Therefore, these reported transformations are probably not related to atomic ordering effects, and their identification requires further experiments.

*In [22], this discussion was performed assuming spin 1/2 for the Fe atoms. A repetition of the calculations with spin 1 did produce slightly modified values, but the conclusions remain valid.

Fig. 8 Complete Phase Diagram of the Fe-Si System

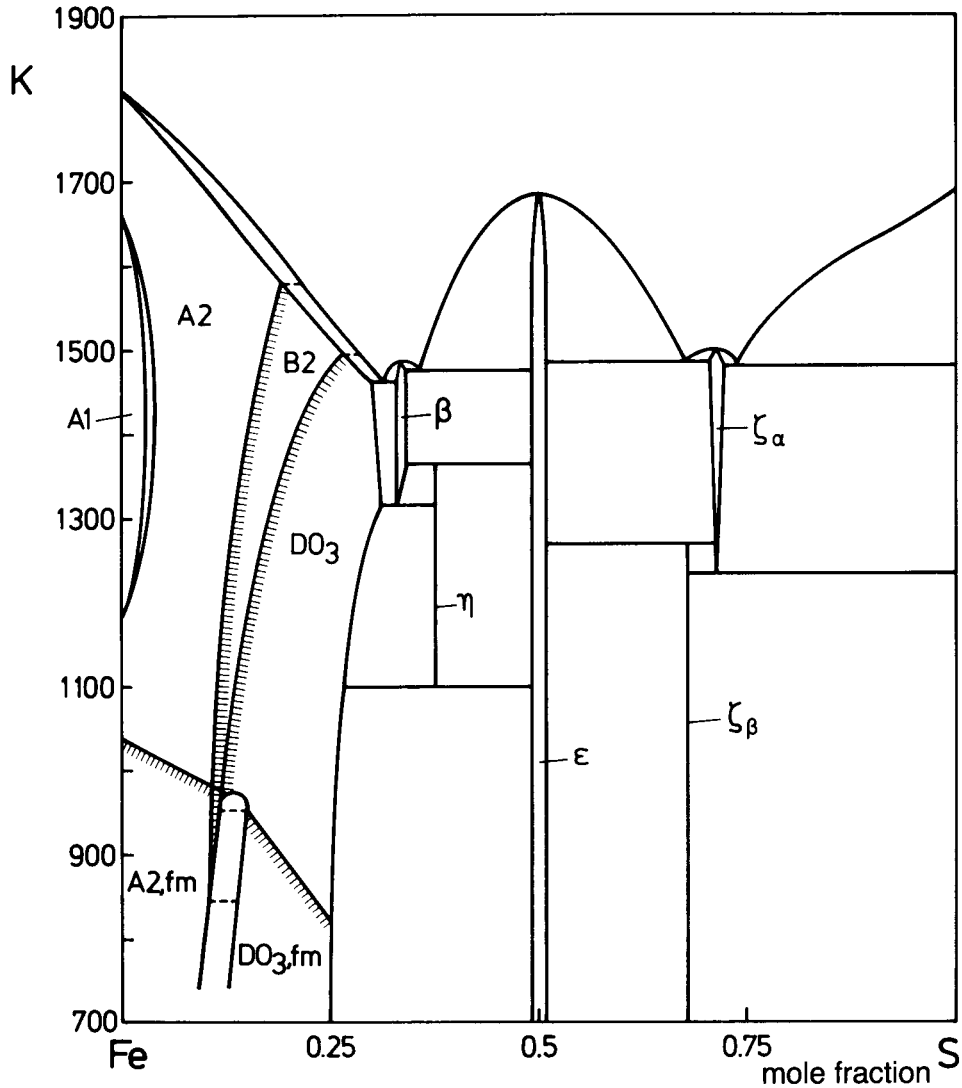

The bcc Equilibria in Fe-Al Alloys. In the bcc Fe-Al alloys, the ordering reactions between first and second nearest neighbors are very similar to those in Fe-Si alloys; the critical temperatures are roughly a factor of two lower. In Fig. 9, the phase diagram is shown up to $x_{Al} = 0.5$. It is based on selected data out of the experimental work in [19] and [31–37]. Particularly in the range where the Curie temperature crosses the critical temperatures of atomic lro, there is considerable scatter in the T_c-data. It is not well established whether or not T_c reaches the miscibility gap $A2 + B2$ at the tricritical point. From Bragg-Williams calculations [38, 39], it has been concluded that the two-phase field $A2 + B2$ is produced by magnetic effects, and therefore, T_c passes through the tricritical point in these calculations. This argument need not be wrong if, in reality, T_c reaches the two-phase field below the tricritical point (as drawn in Fig. 9 according to [31], because magnetic sro also produces magnetic effects above T_c. The two-phase field $A2 + B2$ reported in [33] has been adopted instead of the smaller one reported in [19] because, according to the arguments outlined in [2], the equilibria obtained in [33] are the stable ones, whereas in [19] metastable equilibria have been observed.

Further transformations within the $B2$ field have been reported in [31]. On the basis of the reported data, these additional transformations should be continuous. They have not yet been incorporated in Fig. 9 for reasons already outlined in "The bcc Equilibria in Fe-Si Alloys".

The bcc Equilibria in Fe-Co Alloys. In Fig. 10, the phase diagram for Fe-Co is shown. In the bcc phase field, the ordering reaction $A2 \rightleftarrows B2$ has been observed experimentally [41, 42]. The experiments indicate a continuous transformation. The same result follows from model calculations [43, 44]. Therefore, the critical temperature should be indicated accordingly.

The fcc Equilibria in Co-Ni Alloys. The analysis of heterogeneous equilibria in the vicinity of the Curie temperatures outlined in "Transformations Without Constraint of Homogeneity" has been performed on a hypothetical alloy system with ideal solution behavior. The Co-Ni system is an example that behaves like an ideal solution and exhibits composition-dependent magnetic properties.

Fig. 9 Eclectic Phase Diagram of bcc Fe-Al Alloys with $x_{Al} \leq 0.5$

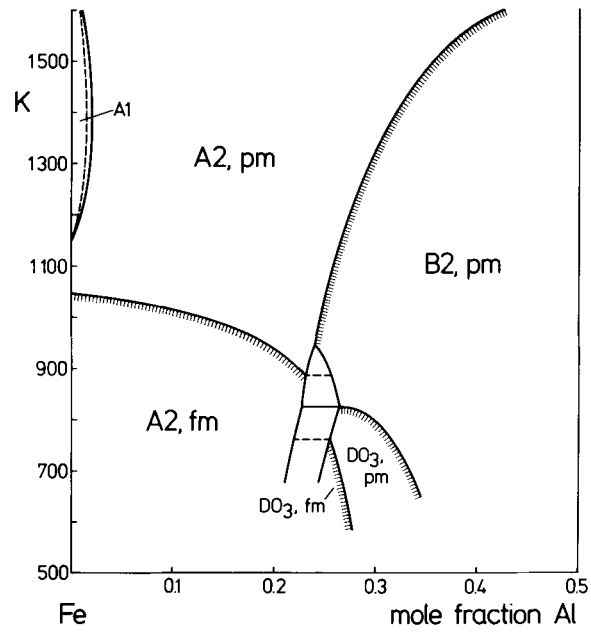

Sources: [19], [31–37].

Fig. 10 Phase Diagram of Fe-Co Alloys

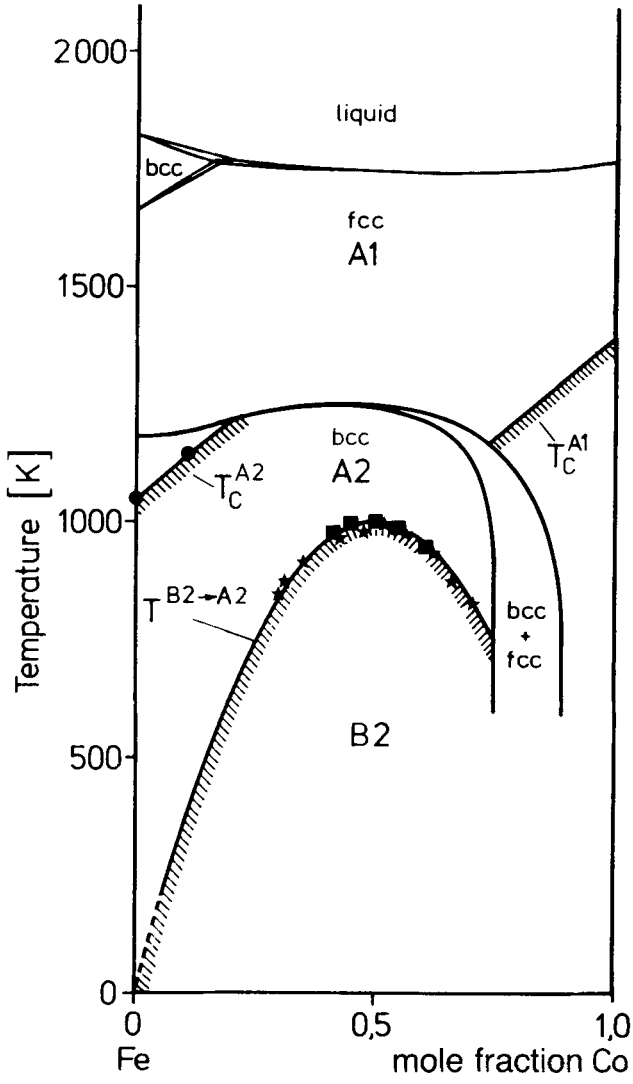

■, ★, ● ≡ Experimental, taken from [40–42].

Fig. 11 Phase Diagram of Co-Ni Alloys [1] and Enthalpy of Formation at T = 1400 K [45]

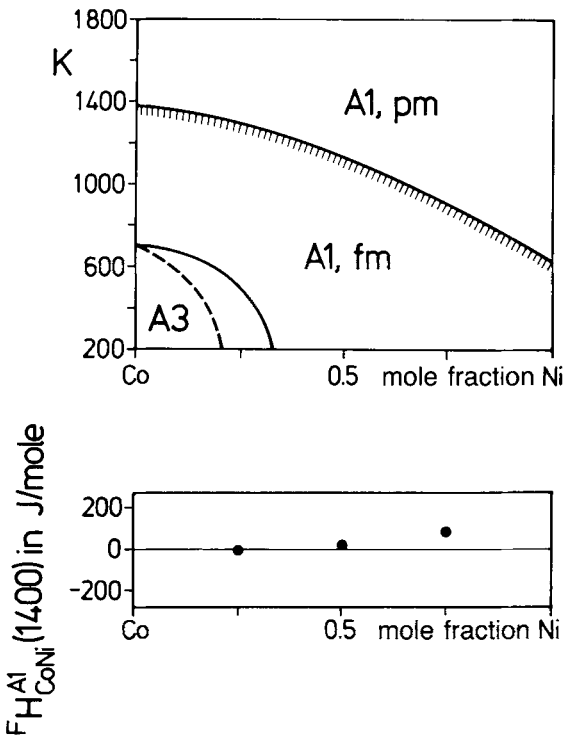

In Co-rich alloys, a transformation from the fcc structure ($A1$) to the cph structure ($A3$) is observed. The calculation of the magnetic effects does not predict heterogeneous equilibria at the Curie temperature.

The ideal solution behavior can be derived from the combination of two experimental facts:*

- The vanishing enthalpy of formation of Co-Ni alloys as represented in the lower part of Fig. 11.
- No atomic long-range order is observed in this system [46–49].

Assuming a linear variation of the mean atomic moment from 1.7 μ_B for Co to 0.6 μ_B for Ni [51], the calculation yields no heterogeneous equilibria in the range of the Curie temperatures, as shown in Fig. 11. The magnetic contributions do not vary enough across the system to produce concave shapes of the Gibbs energy at temperatures close to T_c.

The fcc Equilibria in Co-V Alloys. In the Co-V system, a very strong decrease of the Curie temperature is observed,

*It has been shown in [50] that a vanishing enthalpy of formation is a necessary but usually insufficient condition for ideal solution behavior.

Fig. 12 Magnetically Induced Heterogeneous Equilibria Predicted in the Vicinity of the Curie Temperature in Random fcc (A1) Co-V Alloys

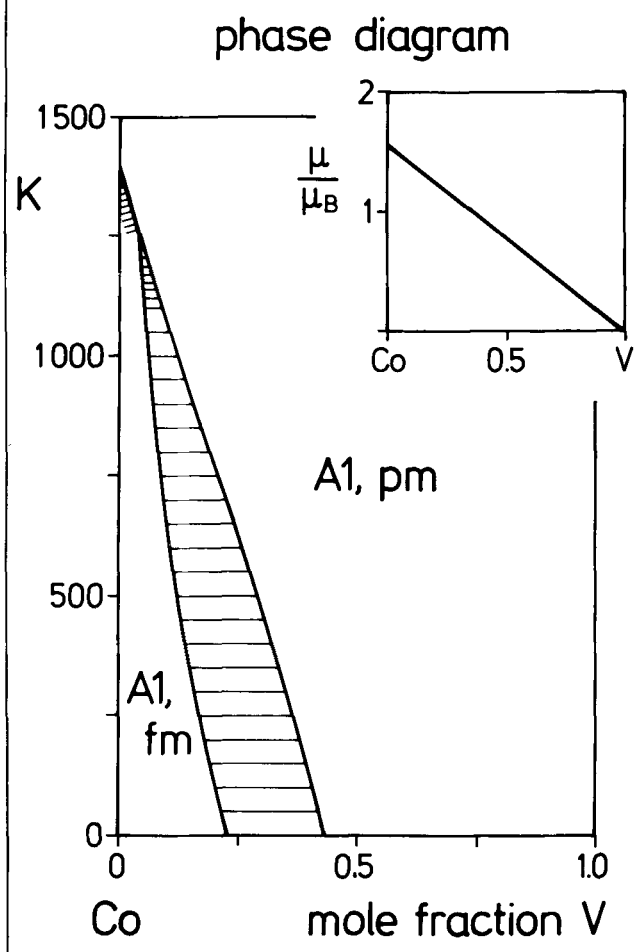

A linear decrease of the Curie temperature with increasing V-content, and the linear decrease of the mean magnetic moment per atom shown in the inset, are presumed in the calculation.

leading to a strong variation of the magnetic contributions across the system. In the paramagnetic state, the random fcc Co-V alloys can be treated as a regular solution [12]. Assuming the composition dependence of T_c as $T_c = 1377 - 4040 \cdot x_V$ [K] and a linear variation of the mean magnetic moment per atom $\mu = 1.7 \cdot x_{Co}$ [μ_B], the calculations yield the phase diagram in Fig. 12. In this instance, heterogeneous equilibria turn out of the calculations. First experimental indications of the existence of such heterogeneous equilibria have been reported in [12] and [52].

References

1. M. Hansen and K. Anderko, *Constitution of Binary Alloys*, McGraw-Hill, New York (1958).
2. S.M. Allen and J.W. Cahn, *Acta Met., 23,* 1017 (1975).
3. D. Landau and E.M. Lifshits, *Statistische Physik*, Akademie Verlag, Berlin (1975).
4. G. Inden, *Acta Met., 22,* 945 (1974).
5. R. Kikuchi and C.M. van Baal, *Scripta Met., 8,* 425 (1974).
6. J. Büth and G. Inden, *Acta Met., 30,* 213 (1982).
7. J.M. Sanchez and D. de Fontaine, *Phys. Rev. B, 21,* 216 (1980).
8. J.L. Meijering, *Philips Res. Repts., 18,* 318 (1963).
9. M. Hillert, Report of the Project Meeting CALPHAD VII, Stuttgart, 80 (1978).
10. T. Nishizawa, M. Hasebe and M. Ko, *Acta Met., 27,* 817 (1979).
11. M. Ko and T. Nishizawa, *J. Jpn. Inst. Met., 43,* 118 (1979).
12. G. Inden, *Physica, 103 B,* 82 (1981).
13. P. Ehrenfest, Proc. Kon. Akad. Amsterdam, *36,* 153 (1933).
14. J.S. Smart, *Effective Field Theories of Magnetism,* Saunders, Philadelphia (1966).
15. E.S.R. Gopal, *Specific Heats at Low Temperatures,* Heywood Books, London (1966).
16. U. Gahn, private communication, accepted for publication in 1982 by *J. Phys. Chem. Solids.*
17. L. Tisza, in *Phase Transformations in Solids,* Smoluchowski, Meyer and Weyl, Ed., Wiley (1951).
18. H.B. Callen, *Thermodynamics,* John Wiley & Sons, New York (1960).
19. P.R. Swann, W.R. Duff and R.M. Fisher, *Met. Trans., 3,* 409 (1972).
20. G. Inden and W. Pitsch, *Z. Metallkunde, 63,* 253 (1972).
21. G. Schlatte and W. Pitsch, *Z. Metallkunde, 66,* 660 (1975).
22. G. Schlatte and W. Pitsch, *Z. Metallkunde, 67,* 462 (1976).
23. G. Inden and W. Pitsch, *Z. Metallkunde, 62,* 627 (1971).
24. G. Inden, *Z. Metallkunde, 66,* 577 (1975).
25. J.A. Hofman, A. Paskin, K.J. Tauer and R.J. Weiss, *J. Phys. Chem. Solids, 1,* 45 (1956).
26. G. Schlatte, G. Inden and W. Pitsch, *Z. Metallkunde, 65,* 94 (1974).
27. P.R. Swann, L. Grånäs and B. Lehtinen, *Metal Science, 9,* 90 (1975).
28. H.-H. Ettwig and W. Pepperhoff, *Z. Metallkunde, 63,* 453 (1972).
29. W. Köster and T. Gödecke, *Z. Metallkunde, 59,* 602 (1968).
30. W. Köster, *Trans. Iron Steel Inst. Jpn., 14,* 387 (1974).
31. W. Köster and T. Gödecke, *Z. Metallkunde, 71,* 765 (1980).
32. W. Pepperhoff, Mannesmann Forschungsinstitut, Duisburg/S.-Germany, private communication.
33. H. Okamoto and P.A. Beck, *Met. Trans., 2,* 569 (1971).
34. K. Oki, H. Sagane and T. Eguchi, *J. de Physique, 38,* C7-414 (1977).
35. H. Sagane, K. Oki and T. Eguchi, *Trans. JIM, 18,* 488 (1977).
36. K. Oki, A. Yamamura, K. Kudo and T. Eguchi, *Trans. JIM, 20,* 451 (1979).
37. G. Inden and W. Pepperhoff, unpublished work.
38. S.V. Semenovskaya, *Phys. Stat. Sol. B, 64,* 291 (1974).
39. H. Sagane and K. Oki, *Trans. JIM, 21,* 11 (1980).
40. W.C. Ellis and E.S. Greiner, *Trans. ASM, 29,* 415 (1941).
41. H. Masumoto, H. Saitô and M. Shonozaki, *Sci. Rep. RITU, 6,* 523 (1954).
42. G. Inden and W.O. Meyer, *Z. Metallkunde, 66,* 725 (1975).
43. T. Eguchi, H. Matsuda and K. Oki, *IEEE Transactions on Magnetics, 4,* 468 (1968).
44. G. Inden, *Z. Metallkunde, 68,* 529 (1977).
45. R. Hultgren, P.D. Desai, D.T. Hawkins, M. Gleiser and K.K. Kelley, *Selected Values of the Thermodynamic Properties of Binary Alloys,* American Society for Metals, Ohio (1973).
46. J.W. Cable, E.O. Wollau, W.C. Köhler and M.K. Wilkinson, *J. Appl. Phys., 33,* 1340 (1962).
47. T.J. Burch, J.I. Budnik and S. Skalski, *J. Phys. Soc. Jpn., 28,* 1180 (1970).
48. A.W. Thompson, *Scripta Met., 8,* 1167 (1974).
49. A.W. Thompson and R.G. Baggerly, *Met. Sci., 9,* 280 (1975).
50. G. Inden, *J. Phys., 38,* C7-373 (1977).
51. E. Vogt, in *Magnetism and Metallurgy,* Vol. 1, A.E. Berkowitz and E. Kneller, Ed., Acad. Press (1969).
52. G. Inden, *Scripta Met., 15,* 669 (1981).
53. M. Hillert and M. Jarl, *Calphad, 2,* 227 (1978).